Effect on the Conformation of a Terminally Blocked, (*E*) β,γ-Unsaturated δ-Amino Acid Residue Induced by Carbon Methylation

Giulia Marafon,[†] Alessandro Moretto,[†,‡,*] David Zanuy,[§] Carlos Alemán,[§,◊] Marco Crisma,[‡] and Claudio Toniolo[†,‡,*]

[†] Department of Chemical Sciences, University of Padova, 35131 Padova, Italy

[‡] Institute of Biomolecular Chemistry, Padova Unit, CNR, 35131 Padova, Italy

[§] Department of Chemical Engineering and Barcelona Research Center in Multiscale Science and Engineering, Universitat Polytècnica de Catalunya, 08019 Barcelona, Spain

[◊] Institute for Bioengineering of Catalonia (IBEC), The Barcelona Institute of Science and Technology, Baldiri Reixac 10-12, 08028 Barcelona Spain

ABSTRACT:

Peptides are well known to play a fundamental therapeutic role and to represent building blocks for numerous useful biomaterials. Stabilizing their active 3D-structure by appropriate modifications remains, however, a challenge. In this study, we have expanded the available literature information on the conformational propensities of a promising backbone change of a terminally blocked δ-amino acid residue, a dipeptide mimic, by replacing its central amide moiety with an (*E*) $C^{\beta}=C^{\gamma}$ alkene unit. Specifically, we have examined by DFT calculations, X-ray diffraction in the crystalline state, and FT-IR absorption / NMR spectroscopies in solution the extended *vs.* folded preferences of analogs of this prototype system either unmodified or possessing single or multiple methyl group substituents on each of its four $-CH_2-CH=CH-CH_2-$ main-chain carbon atoms. The theoretical and experimental results obtained clearly point to the conclusion that increasing the number of adequately positioned methylations will enhance the preference of the original sequence to fold, thus opening interesting perspectives in the design of conformationally constrained peptidomimetics.

INTRODUCTION

Medicinal chemists and pharmacologists openly expressed their request to study synthetic analogues of bioactive peptides with greatly reduced conformational flexibility not before 1970's.[1-3] These compounds were also expected not to be degraded by proteolytic enzymes nor recalcitrant to be transported through model/natural membranes. To this end, conformational restrictions, and sometimes even complete rigidity,[4,5] were envisaged as essential peptide prerequisites for the unambiguous elucidation of their structure – activity relationships. Peptide main-chain changes, involving either α-carbon modifications or amide bond replacements furnished families of compounds (termed peptidomimetics or pesudopeptides)[3,6,7] with significantly enhanced, more favorable physical and biological properties. More recently, it was observed that the enormous rise in the number of publications in this area is not only associated to compounds with therapeutic applications, but related to new properties of peptides in materials science as well.[8-10] In this connection, more than 20 years ago[4,11] it was clearly established that easy insertion of commercially available, achiral ω- (in particular β, γ, and δ-) amino acid residues into α-peptides generates peptidomimetics with replacement of the amide bonds by single or multiple methylene units in their backbones. Interestingly, the number of atoms (six) in a δ-amino acid is precisely matching that of a dipeptide segment. The saturated main chain of δ-amino valeric acid (δ-Ava), or 5-amino-pentanoic acid, reflects with an acceptable approximation that of the Gly-Gly sequence.[10-13] By spectroscopic experiments, X-ray diffraction studies, and energy calculations it was also demonstrated that the simplest, rather flexible δ-Ava residue either prefers a *g-g-t-g-g* torsion angle sequence, thus allowing its accommodation into a folded (helical) peptide conformation, or a more elongated, β-sheet like, 3D-structure, the latter contributing to produce a hydrogel material with nanofibrous morphology at the supramolecular level.[10]

In this perspective, some conformational restrictions to the sp^3 CH_2 carbon chain of ω-amino acids were considered essential to construct appropriate model peptidomimetics with specific 3D-structural stabilizations. The most promising and extensively investigated constraint is the incorporation of a C=C moiety in the backbone. For example: (i) The introduction of one (or multiple, even consecutive) units of the (*E, trans*)/(*Z, cis*) 3-aminoprop-2-enoic acid, -NH-CH=CH-CO-, in a β-peptidomimetic compound allowed its tunable (reversible) photoisomerization between two states, the former (*E*) being more extended and self-associating through N-H…O=C intermolecular H-bonds, while the latter (*Z*) being folded and characterized by a six-membered *pseudo*cycle energetically facilitated by an intramolecular N-H…O=C H-bond.[14,15] (ii) The base-induced double-bond migration of the (*E*) C^{α}=C^{β} moiety to the (*E*) C^{β}=C^{γ} positions of a γ-peptidomimetic, -NH-C^{γ}HR-C^{β}H=C^{α}H-CO- to -NH-C^{γ}R=C^{β}H-$C^{\alpha}H_2$-CO-, results in a conformational change from an open-chain to an intramolecularly H-bonded 3D-structure.[16] (iii) Semi-empirical conformational energy calculations on an (*E*) C^{β}=C^{γ} δ-peptidomimetic showed an increased flexibility with respect to the parent peptide, but *mono*-methylation on the C=C bond was predicted to induce a higher rigidity and a strong preference for backbone folding.[17] Unfortunately, however, subsequent NMR experimental data could not confirm this latter theoretical result.[18] (iv) A fluoroalkene peptide bond isostere (-CF=CH-C-) in which the fluorine atom replaces the peptide carbonyl oxygen in a peptide containing the -Pro-D-Val- sequence was exploited as the catalyst for an epoxidation reaction,[19] and the conformational effects of this type of replacement in connection to the polarizability of the C=O bond were investigated.[20]

Figure 1 illustrates the chemical structures of a set of four N^{δ}-acetylated, C′-methylamidated *E*-olefin dipeptide mimetics (compounds **A** – **D**), exhibiting an (*E*) alkene unit in their main chain. Among *carbon* derivatives, exclusively *methylated* compounds were examined. These derivatives range from the *un*-methylated compound **A**, to the *bis*-methylated compounds **B** and **C** (with *bis*-

methylation either on the C^{β}=C^{γ} double bond, compound **B**, or on the C^{α} / C^{δ} atoms, external to the double bond, compound **C**), to the *ter*-methylated compound **D** (with C^{α}, C^{β}, and C^{δ} methylated atoms). Conformational analyses on terminally-blocked (or protected) analogs of them were already performed to a limited extent by other research groups,[21-24] but their preferred 3D-structures have been re-analyzed in this work, in particular using modern density functional theory (DFT) calculations.

In addition, the present study was aimed at expanding our general knowledge on this peptidomimetic system and studying in detail the conformational preferences of the novel compound **E** (Figure 1) or its N^{δ}-Boc (*tert*-butyloxycarbonyl) protected, *iso*propylamidated analog, **10**, by use of computational analysis, and crystal-state (X-ray diffraction) and solution (FT-IR absorption and NMR spectroscopies) investigations. We consider this dipeptide mimetic, synthetized and studied for the first time, the most important among those investigated in this work because it is characterized by the highest level of carbon methylation. Indeed, our main focus was to further highlight and explain in depth the reasons for the beneficial effect, already suggested in limited cases,[17,21-25] produced by the introduction of methyl substituents on the four internal carbon atoms of the (*E*)-olefin dipeptide mimetic on folding (in particular on formation of the popular β-turns)[26-29] in these peptidomimetics. The most representative β-turns, energetically favored by the occurrence of a C=O…H-N intramolecular H-bond, forming a ten-membered *pseudo*cycle, are the non-helical types I (I′) and II (II′), accompanied by type III (III′), the consecutive repetition of the latter generating the right- (or left-) handed 3_{10}-helical polypeptide structure.[6,30-34]

Finally, for a better comparison, an experimental conformational investigation analogous to that mentioned above for the carbon *tetra*-methylated compound **10** was also carried out on the *un*-methylated compound **6**. Interestingly, the two *gem*-dimethyl groups present in compound **E** make it to closely resemble the homo-dipeptide sequence based on the α-amino acid Aib (α-

aminoisobutyric acid).[32,35,36] Indeed, this sequence, the most prone among those known to adopt a stable type III (III′) β-turn and to afford a regular 3_{10}-helix thanks to a double Thorpe-Ingold effect,[37] is expected to be a very promising choice.

Specifically, here we will discuss in detail the conformational propensities of the *achiral* compounds **A** and **B** *un*-methylated at both -CH_2- ("Gly-Gly" dipeptide mimics) and the *achiral* compound **E** *bis*-methylated at each -CH_2- ("Aib-Aib" dipeptide mimic). In addition, our attention will also focus on the chiral compounds **C** and **D**, both *mono*-methylated at each -CH_2- ("L-Ala-D-Ala" dipeptide mimics).[21-23] The chosen combination of configurations in these two latter compounds corresponds to that which is the most suitable to accommodate the extensively authenticated type-II β-turn conformation in an α-peptide chain. Note that related literature studies on other examples of *chiral* dipeptide mimetics ("Val-Gly",[38] "Leu-Gly",[39] "Ala-Gly",[18] "Phe-Gly",[17] "Phg-Ala",[40] and "Phe-Phe"[41-43]) of this type were not further treated in this paper because these compounds exhibit at least one carbon replacement different from simple methylation.

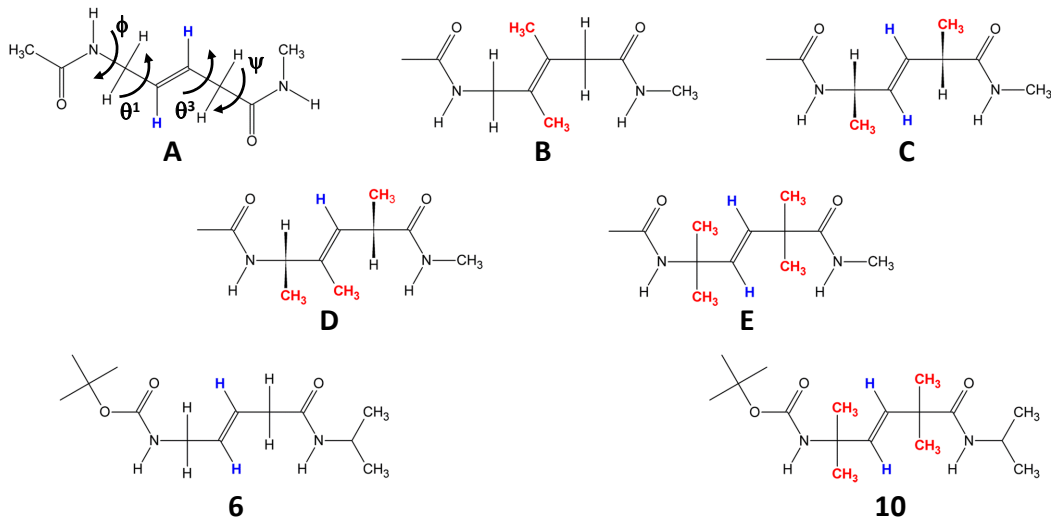

Figure 1. Chemical structures of the compounds investigated in this work either by DFT calculations (compounds **A** – **E**) or experimentally [compounds **6** and **10**]. In **A**, the backbone torsion angles conformationally relevant for this set of compounds are indicated.

RESULTS AND DISCUSSION

Theoretical conformational analysis

A systematic conformational search procedure, which is described in the Experimental Section, was conducted to study the free energy (ΔG) landscape of peptides **A**-**E** (Figure 1) *in vacuo*.

DFT calculations at the M06L/6-31+G(d,p) level on the achiral compounds **A** and **B** led to 9 minimum energy conformations (Supporting Information, Tables S1 and S2, respectively), which are degenerated (*i.e.* minima with $\{\varphi,\theta^1,\theta^3,\psi\}$ and $\{-\varphi,-\theta^1,-\theta^3,-\psi\}$ are energetically equivalent) in a ΔG interval of 4.3 and 4.8 kcal/mol, respectively. However, according to a Boltzmann distribution, only two minima of **A** and one of **B** showed a population higher than 5%. These minima, named **a1** and **a2** in Figure 2a and **b1** in Figure 2b, are stabilized by a specific intramolecular interaction, forming a ten-membered H-bonded ring (C_{10}) that is characteristic of the β-turn.[26-29] Indeed, all these minima mainly differ in the arrangement of the central region, which is defined by the torsion angles θ^1 and θ^3 (Figure 1). In the case of the *un*-methylated **A**, the backbone is slightly more strained for **a2** than for **a1**, improving in the H-bonding geometry but a destabilization of 0.1 kcal/mol. Detailed inspection of Table S1 indicates than such minima present intramolecular H-bonds, whereas the rest do not display any specific interaction. Comparison of these results with the very limited amount of β-turn found by Gellman and co-workers[21,22] in solution for the strictly related N^{δ} *i*Pr-CO-, C′ -NH*i*Pr blocked analog and corroborated by our experimental results on the N^{δ} Boc analog (see below) suggests that the stability of the latter conformations (those without intramolecular H-bonds) increases in condensed phases. In the case of **B**, methylated at both C^{β} and C^{γ}, the backbone torsion angles of **b1** are relatively similar to those of **a2** and, therefore, the H-bonding parameters are close to the ideal geometry. An additional minimum with torsion angles resembling those of **a1** and stabilized by a C_{10} H-bonded ring (Supporting Information, Figure S1)

is also detected for **B**. This 3D-structure results disfavored by 1.8 kcal/mol due to the steric hindrance caused by the side methyl groups.

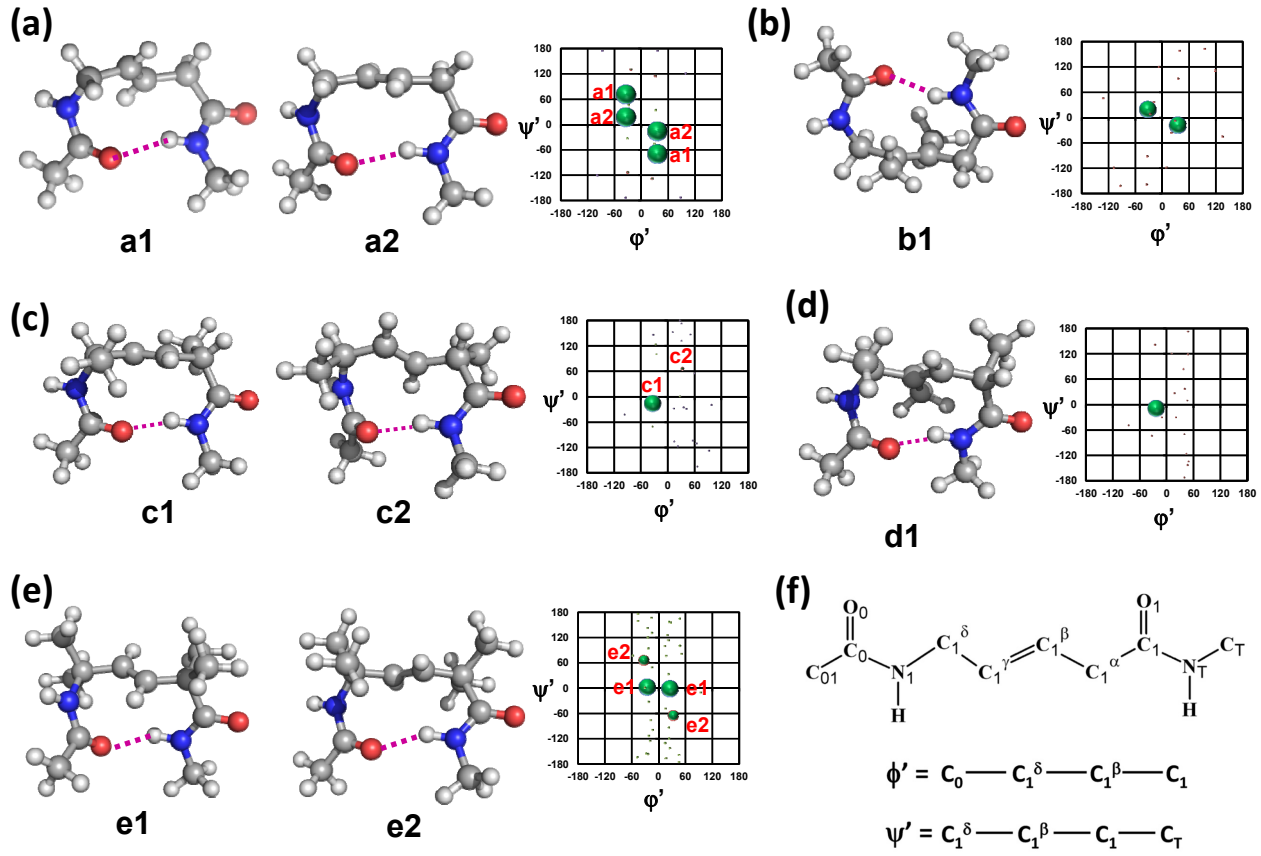

Figure 2. Representative minimum energy conformations and ϕ′,ψ′ maps of compounds **A**, **B**, **C**, **D**, and **E** [(**a**) – (**e**), respectively]. The definition for the ϕ′ and ψ′ virtual torsion angles is given in panel (**f**). In the ϕ′,ψ′ maps, each relevant conformer is represented by a dot of size proportional to its relative population at 298 K. Calculated torsion angles and ΔG values are presented in Tables S1-S5 (Supporting Information).

In order to facilitate the representation of the conformational preferences of **A** and **B**, a Ramachandran-like map was plotted using two virtual torsion angles, φ′ and ψ′ (see Experimental Section, Figure 8), which were selected to account for the relative position of each amide group with respect to the central double bond. The position of all minima was plotted in the maps using dots sized according to ΔG (Figures 2a-b). The map obtained for **A** indicates that both φ′ and ψ′ display low, but non-negligible, conformational flexibilities. This observation explains the very weak band associated to intramolecularly H-bonded N-H that was identified by IR absorption spectroscopy by Gellman and coworkers in solution.[21,22] In contrast, the map depicted for **B** shows that methylation at both C^{β} and C^{γ} atoms causes strong restrictions in the conformational preferences, which is also consistent with previous experimental results[21,22] indicating a significant amount of β-turn in solution.

Energy minimization of the starting conformations constructed for compound **C** (*mono*-methylated at *each* of the C^{δ} and C^{α} atoms to mimic the L-Ala-D-Ala sequence) led to 23 minimum energy conformations, which are listed in Table S3. These minima are distributed in the following way: two minima with $\Delta G \leq 1.5$ kcal/mol, which sum up to a population of 90.7%, while the remaining 21 show $\Delta G_{gp} \geq 1.9$ kcal/mol. The two preferred conformations of **C**, hereafter denoted **c1** and **c2**, are stabilized by a C_{10} H-bond (Figure 2c) and show some resemblance with **a2** and **a1**, respectively. Thus, the substitution of the H atom by a CH_3 group at both C^{δ} and C^{α} atoms inverts the order of stability of the two β-turn folds obtained for **A**. There is an additional conformation stabilized by an intramolecular C_{10} H-bonded ring, named **c6** (Figure S2), which is destabilized by 2.4 kcal/mol (*i.e.*, population at 298 K: 1.3%, Table S3). Inspection of the φ'-ψ' map obtained for **C** (Figure 2c) indicates that methyl substitutions not only alter the energy landscape but also restrict the conformational flexibility with the respect to **A**, favoring considerably the β-turn folding.

Because of its trimethylation (at the C^{δ}, C^{γ}, and C^{α} positions), compound **D** combines the conformational restrictions found for **B** and **C**. The relevant structural parameters of the 18 minimum energy conformations identified for **D** are listed in Table S4. The population of the global minimum amounts to almost 99%, the ΔG of the other minima ranging from 2.8 to 9.4 kcal/mol. The torsion angles of the global minimum (**d1** in Figure 2d), which is stabilized by a C_{10} H-bonded ring, are very similar to those found for **b1**, indicating that the methylation at C^{γ} has a higher influence than that at either C^{α} or C^{δ}. As it is illustrated in the φ'-ψ' map, the contribution of the rest of the minima is practically negligible, even though two of them are stabilized by intramolecular H-bonds. Again, the energy landscape predicted for **D** is fully consistent with the observed preferences for the β-turn conformation.[26-29]

Finally, compound **E**, which is tetramethylated at the C^{α} and C^{δ} atoms, shows 23 degenerated minima (Table S5). However, only two of them, named **e1** and **e2** (Figure 2e), with populations of 74.2% and 25.4%, respectively, are representative. These 3D-structures, which exhibit torsion angles that resemble those of **a2** and **a1**, respectively, are stabilized by a C_{10} H-bonded ring. It is worth noting that the 21 remaining conformers are disfavored by at least 3.9 kcal/mol, strongly suggesting that their contribution in terms of population is practically null.

Overall, our results extracted from DFT calculations indicate that the conformational preferences for the unmethylated **A** are intrinsically constrained by the double bond connecting the C^{β} and C^{γ} atoms. These restrictions increase upon methylation at the sp^2 (C^{β} and C^{γ}) and/or sp^3 (C^{α} and C^{δ}) carbon atoms because of the induced repulsive interactions. The conformational flexibility of **C** decreases with respect to **A** because of $CH_3\cdots H$ interactions, which are much more repulsive than the $H\cdots H$ interactions. The principles of these interactions are analogous to the steric strain balance characteristic of substituted annular compounds (Thorpe-Ingold effect).[37] According to this phenomenon, which was originally extended to peptides by Balaram and coworkers[6] and by

Toniolo and coworkers,[30] the peptide folding can be governed through the restrictions imposed by the incorporation of methyl groups at the sp^3 carbon atoms, as it is observed for **C**. On the other hand, compounds methylated at the sp^2 carbon atoms exhibit the steric 1,3-allylic strain.[21,44] This phenomenon is clearly displayed by **D**, which incorporates a methyl substituent at the *Z* position of the double bond relative to the C^{δ} chiral center. As shown in Tables S3-S4, **D** displays conformational changes with respect to **C** that are caused by the addition of the 1,3-allylic strain to the Thorpe-Ingold effect. The resemblance between the torsion angles of **b1** (1,3-allylic strain), **c1** (Thorpe-Ingold effect), and **d1** (Thorpe-Ingold effect combined with 1,3-allylic strain), which are close to those of **a2** rather than to those of **a1**, suggests that the structural consequences of both repulsive effects are similar.

Amazingly, the conformational behavior of **E** resembles that of **A** more than those of **B**-**D**. Thus, the *bis*-methylation at each of the two sp^3 carbon atoms overrides the effect associated to the steric 1,3-allylic strain, which was observed for **B** and **D**. Moreover, the Thorpe-Ingold effect in **E** results in a slight destabilization of the local minima with respect to **A**, even though the number of minima increases significantly. Thus, the 9 degenerated minima found for **A** are comprised within a ΔG interval of 4.3 kcal/mol, whereas the first 9 minima of **E** are within a range of 4.9 kcal/mol. However, 14 additional local minima, which were not detected for **A**, were identified for **E**. We attribute these features to the fact that the potential surface is more abrupt for **E** than for **A** because the $CH_3\cdots CH_3$ interactions are more repulsive than the H···H interactions. Consequently, the minima are less stable and more numerous in compound **E**. On the other hand, considering that, as mentioned above, Thorpe-Ingold and 1,3-allylic strain effects have a similar impact on the structure and that they are additive, the stability of the β-turn motif should be higher for **E** than for **B**, **C** and, probably, **D**.

Synthesis

The overall synthetic strategy for the preparation of the *un*-methylated compound **6** and its *tetra*-methylated counterpart **10** is illustrated in Scheme 1. Fischer esterification of *trans*-β-hydromuconic acid **1** afforded both the mono- and the diethyl ester derivatives (**2** and **3**, respectively) which were easily separated. Compound **6** was synthesized following essentially the protocol previously reported by Gellman and coworkers.[22] Briefly, the mono-ester **2** was converted into the N^{δ} Boc-protected compound **4** under Curtius rearrangement conditions in the presence of diphenylphosphoryl azide (DPPA), N,N-di*iso*propylethylamine (DIPEA), and *tert*-butanol (*t*BuOH). The subsequent saponification of **4** with LiOH in a water/THF mixture afforded the free acid **5**. Then, C-terminal amination of **5** under 1-hydroxy-1,2,3-benzotriazole (HOBt) / N-(3-dimethylaminopropyl)-N′-ethylcarbodiimide (EDC) mediated coupling with *iso*propylamine provided **6**.

Compound **10** was obtained starting from the diethyl ester of *trans*-β-hydromuconic acid **3** that was tetra-methylated at its acidic methylene positions by treatment with LDA and methyl iodide, yielding **7**. Attempts to carry out a *partial* saponification of **7** to isolate the corresponding mono-acid in an amount large enough to proceed with the synthesis failed. Therefore, we were forced to postpone the de-symmetrization of the molecule to a subsequent synthetic step. *Full* saponification of diester **7** by treatment with LiOH in a water/THF mixture at 0°C afforded the dicarboxylic acid **8.** Mono-amidation of **8** to provide **9** was performed through HOBt/EDC mediated coupling with *iso*propylamine. Then, **9** was converted into the N^{δ} Boc-protected compound **10** under Curtius rearrangement conditions in the presence of DPPA, DIPEA, and *t*BuOH. Workup of the reaction mixture leading to **10** also allowed the isolation of a side product which was identified (*inter alia* by single crystal X-ray diffraction analysis; see below) as the carbamoylazido derivative **11**. The possible formation of such a side product in this type of reaction is documented in the literature.[45]

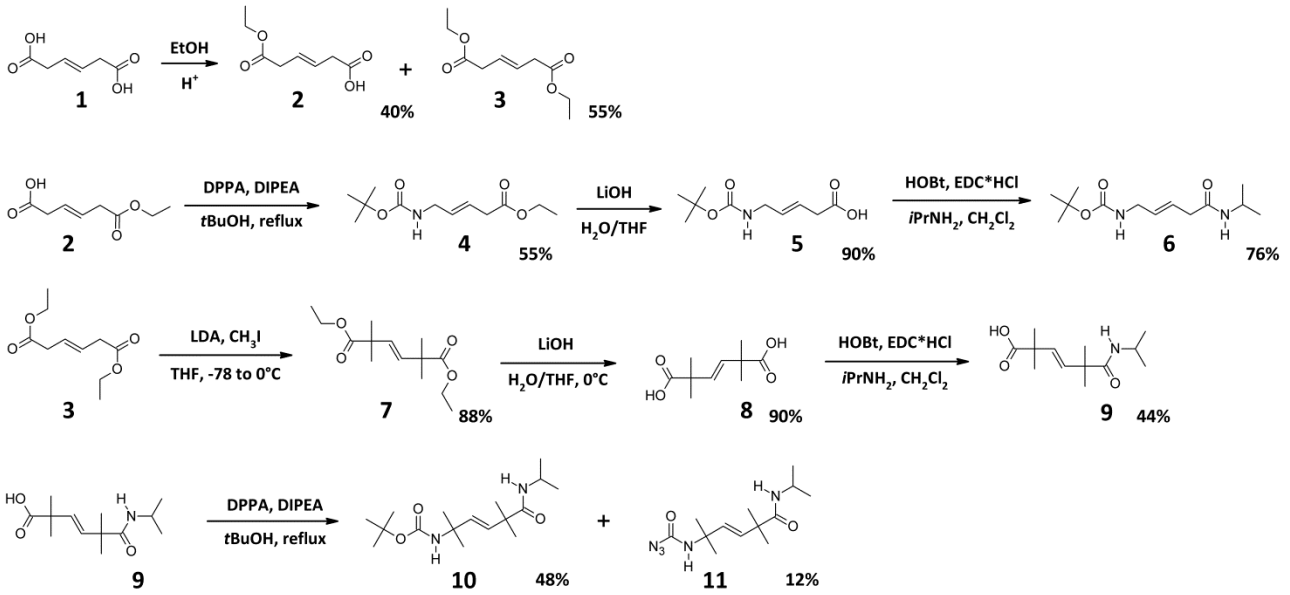

Scheme 1

Crystal-state conformational analysis

The crystal-state conformations of the *un*-methylated compound Boc-5-aminopent-3-(*E*)-enoyl-NH*i*Pr and its *tetra*-methylated analog Boc-5-amino-2,2,5,5-tetramethyl-pent-3-(*E*)-enoyl-NH*i*Pr (compounds **6** and **10**, respectively, in Scheme 2) were determined by X-ray diffraction analysis. In addition, the N^{δ}-azidocarbonyl analog of compound **10** (denoted as **11** in Scheme 2 and obtained as a minor side product in the synthesis of **10**) was also characterized by single crystal X-ray diffraction analysis. In general, bond distances and bond angles are in agreement with values typical for the Boc-urethane group,[46] the alkene and azido moieties,[47] and the amide unit.[48] In all three structures the -C-CH=CH-C- moiety is found in the expected *E* disposition, with deviations from the *trans* planarity not exceeding 4.7°. The urethane and amide bonds are also found in the *trans* disposition, the largest deviation [12.59(16)°] from 180° being found for ω^{N} of molecule 3 in the structure of Boc-5-aminopent-3-(*E*)-enoyl-NH*i*Pr (**6**).

Three crystallographically independent molecules compose the asymmetric unit in the structure of Boc-5-aminopent-3-(*E*)-enoyl-NH*i*Pr (**6**) (Figure 3) in the monoclinic centrosymmetric

space group C2/c. The values of the backbone torsion angles (Supporting Information, Table S9) adopted by the three molecules indicate that molecules 1 and 2 have in common a succession of similar ϕ, θ^1, and θ^3 values [141.8(2)°, 119.8(3)°, and -121.2(3)°, respectively, in molecule 1, whereas 140.2(2)°, 125.6(2)°, and -117.9(3)° in molecule 2], but differ by almost 20° in the value of ψ [-123.2(2)° *vs.* -142.2(2) °]. Overall, molecules 1 and 2 are essentially extended.

The conformation adopted by molecule 3 is more kinked at the ϕ level [87.9(2)°], while the remaining θ^1, θ^3, and ψ torsion angles [127.4(2)°, -107.4(2)°, and -138.7(2)°, respectively] are not far from those of the other two molecules. As a consequence of the (more or less) extended backbone conformation, all molecules are devoid of any intramolecular H-bond. Conversely, an extended network of intermolecular N-H…O=C H-bonds is observed in the packing mode (Supporting Information, Table S10 and Figure S4). Each molecule is involved in four intermolecular H-bonds with two flanking molecules (either within the same asymmetric unit or symmetry related), on one side as the donor [through the N-terminal (N) and the C-terminal (NT) N-H groups] and on the other side as the acceptor (through the urethane O0 and the C-terminal O carbonyl oxygen atoms).

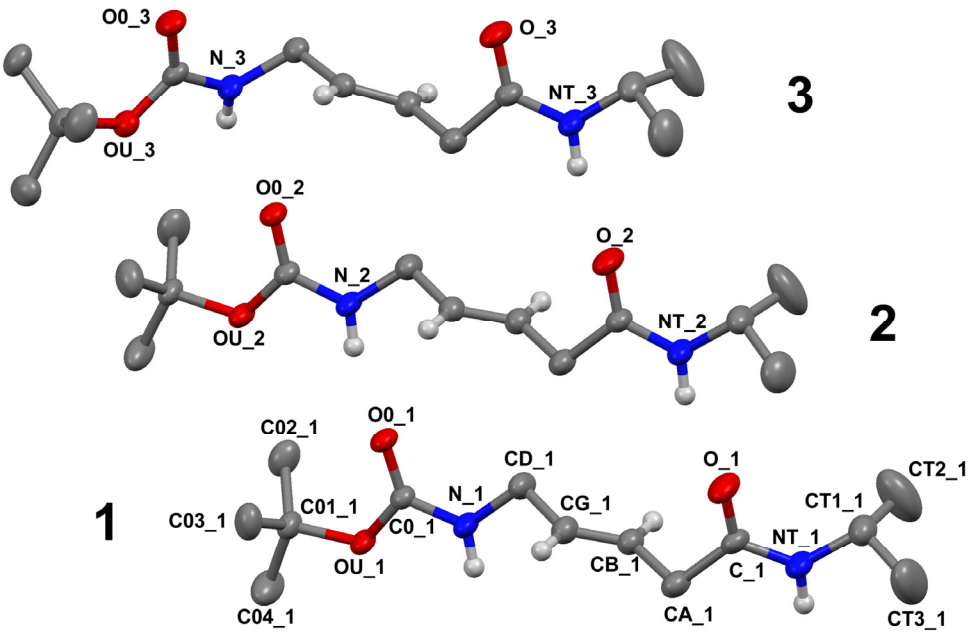

Figure 3. X-Ray diffraction structure of Boc-5-aminopent-3-(*E*)-enoyl-NH*i*Pr (6). The three crystallographically independent molecules are labeled 1, 2, and 3, respectively. Only nitrogen and oxygen atoms are numbered, except for molecule 1 for which full atom numbering is reported. Anisotropic displacement ellipsoids are drawn at the 30% probability level. Most of the H-atoms are omitted for clarity.

At variance with its *un*-methylated counterpart described above, Boc-5-amino-2,2,5,5-tetramethyl-pent-3-(*E*)-enoyl-NH*i*Pr (**10**) adopts a folded conformation in the crystal state (Figure 4), stabilized by an intramolecular N-H…O=C H-bond between the C-terminal *iso*propylamide NT-H group and the urethane carbonyl O0 oxygen atom [N…O and H…O distances 3.120(3) Å and 2.30 Å, respectively; N-H…O angle 160.6°].[49-52] In the molecule arbitrarily selected as the asymmetric unit in this centrosymmetric structure, the values of the ϕ, θ^1, θ^3, and ψ torsion angles are 60.4(3)°, 8.9(4)°, 98.7(3)°, and -3.3(3)°, respectively. These values are not far from the backbone torsion angles typical for the *i*+1 and *i*+2 corner positions of a regular type-I′ β-turn conformation (60°, 30° and 90°, 0°, respectively).[26-29] Interestingly, the near-zero value of θ^1 allows the staggering of the C1G-H bond relative to the two methyl substituents on C1D. As a result, the (ethylenic) H-atom linked to C1G is at 2.62 Å from C1D1 and 2.80 Å from C1D2. Similarly, as a consequence of the value of ψ, the C1=O1 group is staggered with respect to the C1A1 and C1A2 methyl groups.

In the packing mode, an intermolecular H-bond is observed between the (urethane) N1-H1 group and a (*x*, *y*-1, *z*) translational equivalent of the (amide) O1 carbonyl oxygen atom, generating rows of molecules (of the same handedness within each row) along the *b* direction (Supporting Information, Table S12 and Figure S6). Packing is then completed through van der Waals interactions.

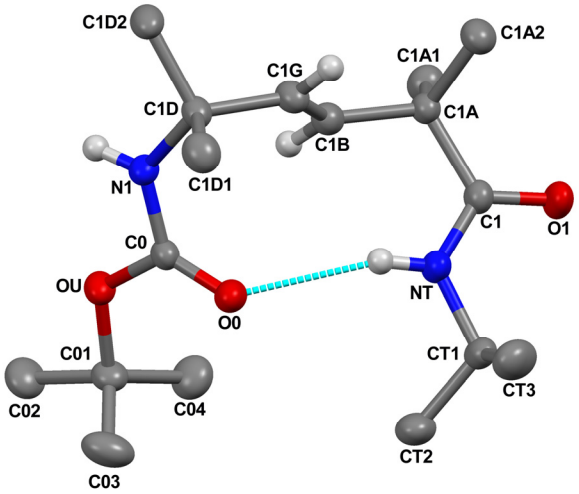

Figure 4. X-Ray diffraction structure of Boc-5-amino-2,2,5,5-tetramethyl-pent-3-(*E*)-enoyl-NH*i*Pr (**10**). Anisotropic displacement ellipsoids are drawn at the 30% probability level. Most of the H-atoms are omitted for clarity. The (urethane) C=O…H-N (amide) intramolecular H-bond is represented by a dashed line.

The crystal-state conformation of azidocarbonyl-5-amino-2,2,5,5-tetramethyl-pent-3-(*E*)-enoyl-NH*i*Pr (**11**) (Figure 5) is also folded and stabilized by an intramolecular H-bond between the C-terminal *iso*propylamide NT-H group and the carbonyl O0 oxygen atom [N…O and H…O distances 3.0641(15) Å and 2.25 Å, respectively; N-H…O angle 158.7°].[49-52] The values of the backbone torsion angles of the molecule arbitrarily selected as the asymmetric unit in the centrosymmetric structure are: ϕ = 50.7(2)°, θ^1 = -130.52(15)°, θ^3 = -110.48(15)°, and ψ = 32.42(17)°. Therefore, at variance with the Boc-analog **10** described above, the folding of **11** resembles that of a type-II′ β-turn,[26-29] in which the typical ϕ,ψ values for the *i*+1 and *i*+2 corner positions are 60°,-120° and -80°,0°. Basically, the main difference in the backbone folding between **10** and **11** is represented by a 180° flipping of the central ethylenic unit. As a result, in the structure

of **11**, the (ethylenic) C1G-H bond is *anti*-periplanar to the C1D-C1D1 bond, thus bringing the H-atom linked to C1G closer to C1D2 (2.76 Å) than to C1D1 (3.37) Å.

The packing mode of **11** is similar to that of **10**, being characterized by an intermolecular H-bond between the N1-H1 group and a (*x*, *y*-1, *z*) translational equivalent of the O1 carbonyl oxygen atom, generating rows of molecules along the *b* direction (Supporting Information, Table S14 and Figure S7).

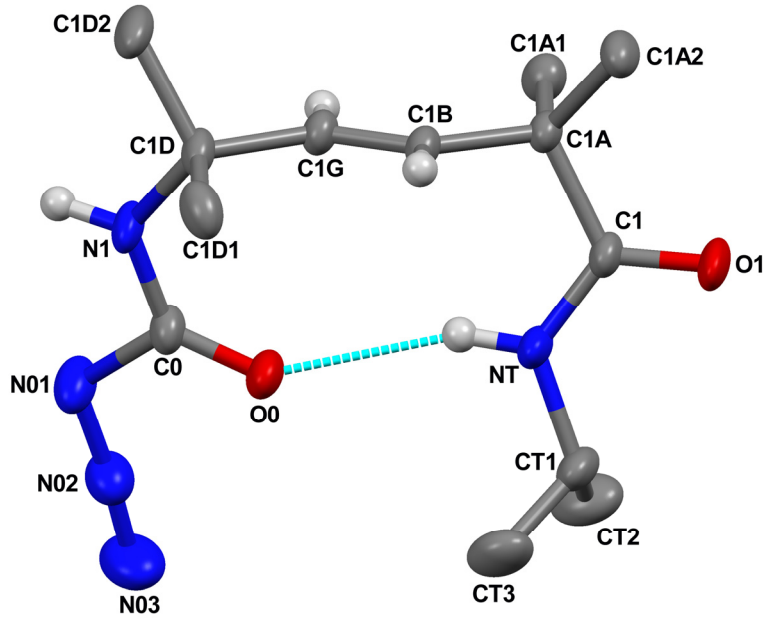

Figure 5. X-Ray diffraction structure of azidocarbonyl-5-amino-2,2,5,5-tetramethyl-pent-3-(*E*)-enoyl-NH*i*Pr (**11**). Anisotropic displacement ellipsoids are drawn at the 30% probability level. Most of the H-atoms and the second position for the methyl groups of the disordered C-terminal isopropyl group are omitted for clarity. The (carbamoylazido) C=O…H-N (amide) intramolecular H-bond is represented by a dashed line.

The different β-turn-like conformations adopted by **10** and **11**, namely type-I′ (I) in **10**, whereas type-II′ (II) in **11**, might at least in part be related to the different packing requirements associated to the N-terminal groups (Boc in **10** *vs.* azidocarbonyl in **11**). In any case, it is clear that both conformations are accessible to the -CO-NH-C(CH_3)$_2$-CH=CH-C(CH_3)$_2$-CO-NH- sequence. Interestingly, the results of the gas-phase DFT calculations on the related compound **E** (Figure 1) indicate as the most stable and most populated (74.2% at 298 K) conformation that characterized by φ, θ^1, θ^3, and ψ values for the backbone torsion angles of 58.1°, -125.8°, -107.4°, and 23.8°, respectively (conformer **e1** in Figure 2; see also Supporting Information, Table S5). These values are close to those found in the structure of **11**. In addition, the conformer **e2** (Figure 2 and Supporting Information, Table S5), which is only 0.6 kcal/mol above the global minimum, with a population of 25.4% *in vacuo* at 298 K according to the theoretical results, exhibits backbone torsion angles (φ, θ^1, θ^3, ψ = 60.4º, 8.8º, 98.6º, -3.2º) not far from those observed in the structure of **10**.

It is worth mentioning that a recent study on a series of tetrapeptide-based organocatalysts, mosty based on a central -D-Pro-Xxx- sequence (where Xxx is a C^α-tetrasubstituted residue), reported examples of a given compound exhibiting either type-I′ or II′ β-turn crystal-state conformations in different polymorphs or pseudopolymorphs.[53] In our case, however, the different crystal-state conformations adopted by compounds **10** and **11** cannot be ascribed to solvent-driven nucleation effects, since crystals of both compounds were grown from ethyl acetate – petroleum ether by vapor diffusion.

Conformational analysis in solution

To obtain information on the tendency toward intramolecularly H-bonded, folded 3D-structure formation of the *un*-methylated "Gly-Gly" dipeptide mimic compound **A** and its *tetra*-

methylated "Aib-Aib" dipeptide mimic compound **E**, both achiral, we carried out FT-IR absorption and ^{1}H NMR investigations in $CDCl_3$ solution on their more soluble, N^{δ}-Boc protected, C′-*iso*propylamide analogs **6** and **10** (Figure 1).

In the FT-IR absorption spectra [amide A (N-H stretching) region] (Figure 6), the bands (shoulders) above 3415 cm^{-1} for the two compounds are assigned to the free (solvated) urethane and amide NH groups, while the band near 3358 cm^{-1} to C=O…H-N H-bonded NH groups.[54-57] The ratio of the integrated intensity of the free / H-bonded bands is hugely in favor of the free spectral component in the case of **6**, whereas the H-bonded spectral component is even prevailing in the case of **10**. Moreover, this ratio changes, but slightly, for (Boc)**A 6**, whereas it remains remarkably unmodified for **10** upon a tenfold dilution (from 1.0 to 0.1 mM concentration; Supporting Information, Figures S8 and S9). This finding strongly suggests that the observed H-bonding is essentially *intra*molecular in the case of **10**, while intermolecular H-bonds contribute, but only to some extent, to the weak H-bonded band of **6**. These results, in excellent agreement with those already published by Gellman and coworkers[21,22] on an N^{δ}-acylated analog of **A** and one of its *bis*-methylated derivatives in DCM solution, clearly support the view that there is very little intramolecular H-bonding in this backbone structure in the absence of significant methylation and of the related preorganization induced by either allylic strain[44] (as in the Gellman's β,γ *bis*-methylated derivative) or the double Thorpe-Ingold effect operative in our compound **10**, *gem*-dimethylated at both C^{α} and C^{δ}. From these IR absorption data we also tend to conclude, again in parallel to refs. 21 and 22, that the almost exclusive type of intramolecular H-bond in compound **10** refers to that with the C-terminal amide NH group as donor and the N-terminal urethane C=O group as acceptor (formation of the common C_{10}- or β-turn) as observed in the crystal state (see above), without any relevant contribution from the rather unusual C_8- or δ-turn[58] formation (with the N-terminal urethane NH group as donor and the C-terminal amide C=O group as acceptor). Finally, it

is worth emphasizing that the H-bonded spectral component is significantly larger in our *tetra*-methylated compound **10** than in the Gellman's β,γ *bis*-methylated compound (labeled **1** in ref. 21 and **2** in ref. 22).

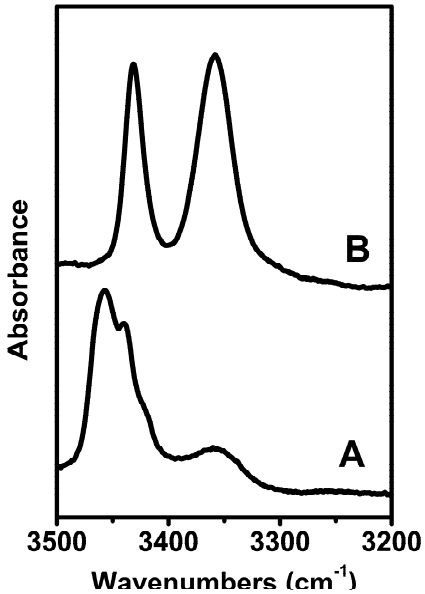

Figure 6. FT-IR absorption spectra in $CDCl_3$ solution (1.0 mM concentration) of compounds **6** (A) and **10** (B) in the 3500-3200 cm^{-1} wavenumber (N-H stretching) region.

Our FT-IR absorption conclusions on the conformational preferences of **10** in $CDCl_3$ solution at 1.0 mM concentration were confirmed by a 400 MHz ^1H NMR investigation. The delineation of intramolecularly H-bonded NH group(s) was carried out by use of solvent dependence of NH proton chemical shifts by adding increasing amounts of the strong H-bonding acceptor solvent DMSO[59] to the $CDCl_3$ solution (Figure 7). The upfield resonance in $CDCl_3$ (5.2 ppm) is unambiguously assigned to the N-terminal urethane NH proton.[55] This NH resonance is remarkably sensitive to the addition of DMSO, whereas the other (amide) resonance displays a behavior suggesting insensitivity of the chemical shift to solvent composition. In summary, our ^1H

NMR results allow us to reasonably conclude that in a solvent of low polarity ($CDCl_3$) and in the absence of self-association the C-terminal *iso*propylamide NH proton is almost inaccessible to the perturbing agent and is therefore most probably intramolecularly H-bonded.

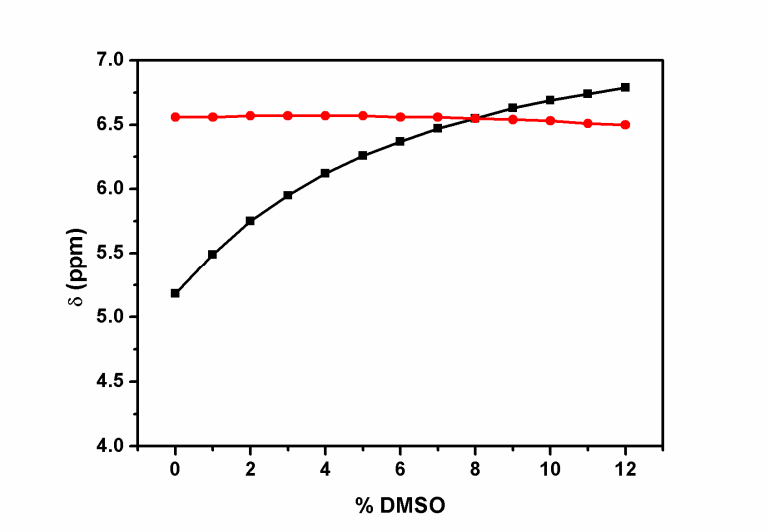

Figure 7. Plot of the chemical shifts of the NH proton signals in the NMR spectrum of Boc-5-amino-2,2,5,5-tetramethyl-pent-3-(*E*)-enoyl-NH*i*Pr (**10**) as a function of the addition of increasing percentages (*v*/*v*) of deuterated DMSO to the $CDCl_3$ solution. Peptide concentration: 1.0 mM. The Boc-urethane and the C-terminal *iso*propylamido NH proton signals are displayed in black and red colors, respectively.

CONCLUSIONS

(*Trans*) amide-to-(*E*) olefin is an ideal replacement in a peptide because both the overall geometrical and conformational preferences of the former backbone are essentially maintained in the latter. In particular, the number of intervening atoms in the saturated -$C^{\delta}H_2$-$C^{\gamma}H_2$-$C^{\beta}H_2$-$C^{\alpha}H_2$- δ-amino acid δ-Ava corresponds exactly to that in the "original" -Gly-Gly- dipeptide sequence. As a result, not surprisingly in recent years the conformational propensities of terminally blocked (or

protected) δ-Ava analogs with a central (*E*) olefin moiety have been the subject of a few investigations.[17,18,21-24,38-43] However, their potentially large variety has been covered only partially and the conclusions extracted appear sometime contradictory.

In this work, we focused our DFT computational and experimental (X-ray diffraction, FT-IR absorption, and NMR) studies on the conformation of the -NH-CH_2-CH=CH-CH_2-CO- system of β,γ-olefin δ-Ava derivatives with only simple methyl substitutions on its carbon atoms, including the hitherto unexplored *bis*-methylation at each -CH_2- (in addition to the unsubstituted sequence). The obtained in-depth information on the 3D-structural preferences (specifically, on the folding tendencies) confirm the initial findings by Gellman,[21,22] Wipf[23] and their coworkers of the role of the allylic 1,3-strain[44] as a favorable controlling 3D-structural factor in inducing β-turn formation. However, the most relevant piece of additional information comes from our investigation on the (2,2,5,5) *tetra*-methylated derivative which exhibits the remarkably highest tendency to fold known so far in this series, primarily promoted by a Thorpe-Ingold effect[7,37] (double *gem*-methylation). Interestingly, the X-ray diffraction data clearly highlight the propensity of the *tetra*-methylated -NH-C(CH_3)$_2$-CH=CH- C(CH_3)$_2$-CO- system studied in this work to access both most classical types, either I (I′) or II (II′), of β-turns. Taken together, our results suggest that the stability of the β-turn pattern of the -CH_2-CH=CH-CH_2- sequence of a β,γ-unsaturated *E*-olefin dipeptide mimetic might be even further enhanced in the case of the completely (hexa-) methylated system.

EXPERIMENTAL SECTION

General Information. The HPLC measurements were performed using an Agilent 1200 apparatus, equipped with a UV detector at 216 nm and a column Agilent extend-C18 (stationary phase). Eluants: A= 9:1 H_2O/CH_3CN, 0.05 % TFA; B= 1:9 H_2O/CH_3CN, 0.05 % TFA. ^1H NMR, ^{13}C NMR, and 2D-NMR spectra were recorded at 25°C on a Bruker Avance 400 MHz instrument. ^1H and ^{13}C spectra were referenced relative to the solvent residual peaks and chemical shifts (δ) are reported in ppm downfield of tetramethylsilane [$CDCl_3$ δ H: 7.26 ppm, δ C: 77.16 ppm; DMSO (dimethylsulfoxide) δ H: 2.50 ppm]. The multiplicity of a signal is indicated as br, broad; s, singlet; d, doublet; t, triplet; m, multiplet. Mass spectra by electrospray ionization (ESI), collected in the positive mode, were performed on a Perseptive Biosystem Mariner ESI-ToF5220 spectrometer. FT-IR absorption spectra were recorded with a Nicolet Nexus FT-IR spectrometer, nitrogen flushed, equipped with a sample-shuttle device. The KBr disk technique was used for the characterization of solid compounds, while oily products were placed between two KBr windows. The frequency maxima for the main absorption bands are given. FT-IR absorption spectra in $CDCl_3$ (99.8%, *d*) solution were recorded at 293 K, averaging 100 scans. Solvent (baseline) spectra were obtained under the same conditions. For spectral elaboration, the software SpectraCalc, provided by Galactic (Salem, MA) was employed. Cells with path lengths of 1.0 mm and 10.0 mm (with CaF_2 windows) were used. Column chromatography was performed on 230−400 mesh silica gel.

DIPEA, *trans*-β-hydromuconic acid, lithium hydroxide hydrate, lithium diisopropylamide solution (LDA, 2.0 M in THF/heptane/ethylbenzene), methyl iodide, DPPA, glacial acetic acid, EDC hydrochloride, isopropylamine (*i*Pr-NH_2), ethanol (EtOH), *tert*-butanol (*t*BuOH), diethyl ether (Et_2O), CH_3CN, TFA, DCM, EA, THF, deuterated $CDCl_3$, and deuterated DMSO were obtained from Sigma-Aldrich and used without further purification. HOBt was purchased from GL Biochem (Shanghai, China).

Synthesis and Characterization of Compounds

Compounds 2 [5-ethoxycarbonyl-3-(*E*)-pentenoic acid] and 3 [hex-3-(*E*)-enedioic acid diethyl ester].[22] Commercially available *trans*-β-hydromuconic acid (**1**) (5 g, 34.7 mmol) was dissolved in 30 mL of anhydrous EtOH. To this solution two drops of concentrated H_2SO_4 were added, and the mixture was heated under reflux for 3 h. After cooling the reaction mixture to room temperature, the solvent was removed under reduced pressure. The reaction crude was dissolved in diethyl ether (Et_2O) and washed with $NaHCO_3$ (5%) and brine. The organic layer was dried with Na_2SO_4 and filtered. Pure compound **3** was obtained as a colorless oil after evaporation of Et_2O (3.8 g, 19 mmol, 55%). The aqueous basic solution was acidified with solid $KHSO_4$ and extracted with Et_2O. The solution was dried over Na_2SO_4, filtered, and concentrated to dryness. Compound **2** was obtained as a colorless waxy solid (2.39 g, 13.9 mmol, 40%).

Compound 2: ^{1}H NMR (400 MHz, $CDCl_3$) δ 7.54 (br, 1H), 5.74 – 5.48 (m, 2H), 4.06 (q, J = 7.1 Hz, 2H), 3.00 (d, J = 5.0 Hz, 4H), 1.18 (t, J = 7.1 Hz, 3H) ppm. IR (KBr) ν (cm^{-1}) 2984, 2901, 1737, 1710, 1691, 1401, 1293, 1218, 1157. MS (ESI) calcd for $C_8H_{13}O_4^+$ $[M+H]^+$ *m/z* 173.0808, found 173.0966.

Compound 3: ^{1}H NMR (400 MHz, $CDCl_3$) δ 5.78 – 5.63 (m, 2H), 4.15 (q, J = 7.1 Hz, 4H), 3.09 (dd, J = 3.7, 1.3 Hz, 4H), 1.27 (t, J = 7.1 Hz, 6H) ppm. IR (KBr) ν (cm^{-1}) 2983, 2939, 1737, 1371, 1275, 1249, 1177, 1158. MS (ESI) calcd for $C_{10}H_{17}O_4^+$ $[M+H]^+$ *m/z* 201.1121, found 201.1308.

Compound 4 [ethyl-5-t-butoxycarbonylaminopent-3-(*E*)-enoate].[22] Compound **2** (1.0 g, 5.8 mmol) was dissolved in dry THF and cooled with an ice bath. DIPEA (1.0 mL, 5.8 mmol) and DPPA (1.25 mL, 5.8 mmol) were added, and the solution was stirred for 30 min. Then, the ice bath was removed and the solution was allowed to reach room temperature. *t*-BuOH (15 mL) was added and the reaction was stirred under reflux overnight. The solvent was removed under reduced pressure and the residue dissolved in EA. The organic phase was washed with $KHSO_4$ (5%),

$NaHCO_3$ (5%) and brine, dried over Na_2SO_4, filtered, and concentrated to dryness. The crude product was purified by flash chromatography (eluant: 1:3, EA/hexane) to give 0.78 g (3.19 mmol, 55%) of **4** as a colorless oil.

^1H NMR (400 MHz, $CDCl_3$) δ 5.81 – 5.51 (m, 2H), 4.63 (br, 1H), 4.14 (q, J = 7.1 Hz, 2H), 3.74 (t, 2H), 3.06 (d, J = 6.8 Hz, 2H), 1.45 (s, 9H), 1.27 (d, J = 7.1 Hz, 2H) ppm. 13C{1H} NMR (101 MHz, $CDCl_3$) δ 171.5, 155.7, 130.7, 123.7, 60.6, 42.1, 37. 6, 28.3, 14.1 ppm. IR (KBr) ν (cm^{-1}) 3364, 2979, 2931, 1737, 1715, 1518, 1366, 1249. MS (ESI) calcd for $C_{12}H_{22}NO_4^+$ $[M+H]^+$ *m/z* 244.1543, found 244.1701.

Compound 5 [5-[N-(tert-butyloxycarbonyl)amino]-pent-3-(*E*)-enoic acid].[22] Compound **4** (0.6 g, 2.5 mmol) was dissolved in THF (10 mL) and $LiOH{\cdot}H_2O$ (0.17 g, 3.9 mmol), dissolved in water (10 mL), was added dropwise. The reaction was followed by TLC. After formation of the mono-ester (observed by TLC), the mixture was acidified with solid $KHSO_4$, and extracted with EA. The organic phase was dried over Na_2SO_4, filtered and concentrated to dryness. The crude product was purified by flash chromatography (eluant: 2:1, EA/hexane) to give 0.477 g (2.22 mmol, 90%) of **5** as a colorless oil.

MS (ESI) calcd for $C_{10}H_{18}NO_4^+$ $[M+H]^+$ *m/z* 216.1230, found 216.1392.

Compound 6 [isopropyl 5-[N-(tert-butyloxycarbonyl)amino]-pent-3-(*E*)-enamide].[22] Compound **5** (1.0 g, 4.6 mmol) was dissolved in dry CH_3CN and HOBt (0.63 g, 4.6 mmol) and EDC·HCl (0.89 g, 4.6 mmol) were added. After 15 min *i*Pr-NH_2 (474 µL, 5.52 mmol) was added to the reaction mixture, and DIPEA was used to reach basic pH. The reaction was allowed to stir overnight. The solvent was removed under reduced pressure and the residue dissolved in EA. The organic phase was washed with $KHSO_4$ (5%), $NaHCO_3$ (5%) and brine, dried over Na_2SO_4, filtered,

and concentrated to dryness. The crude product was purified by flash chromatography (eluant: 1:3, EA/hexane) to give 0.89 g (3.5 mmol, 76%) of **6** as a colorless solid.

Mp 118-120°C (lit. 116-119°C)[20]. ^{1}H NMR (400 MHz, $CDCl_3$) δ 5.76 – 5.54 (m, 3H), 4.76 (br, 1H), 4.12 – 4.01 (m, 1H), 3.73 (t, J = 5.3 Hz, 2H), 2.94 (d, J = 6.9 Hz, 2H), 1.45 (s, 9H), 1.15 (d, J = 6.6 Hz, 6H) ppm. 13C{1H} NMR (101 MHz, $CDCl_3$) δ 169.9, 155.9, 131.8, 124.7, 42.3, 41.4, 40.1, 28.4, 22.6 ppm. IR (KBr) ν (cm^{-1}) 3349, 3308, 2973, 1683, 1641, 1529. MS (ESI) calcd for $C_{13}H_{25}N_2O_3^+$ $[M+H]^+$ *m/z* 257.1860, found 257.2018.

Compound 7 [diethyl 2,2,5,5-tetramethylhex-3-(*E*)-enedioate]. Compound **3** (5.0 g, 24.9 mmol) was dissolved in dry THF, and cooled at -78°C. Then, Ar was fluxed in a three-neck round-bottom reaction flask. LDA (2M in THF, 25 mL, 50 mmol) was added to the solution. After 30 min CH_3I (3.11 mL, 50 mmol) was added at -78°C and the reaction mixture was stirred for 3 h at room temperature. The mixture was diluted carefully with an aqueous solution of $KHSO_4$ (6.8 g, 50 mmol) and extracted with EA. The organic layer was additionally washed with $KHSO_4$ (5%), $NaHCO_3$ (5%), and brine, dried over Na_2SO_4, filtered and concentrated to dryness. After the work up, the alkylation procedure was repeated using the same quantities of LDA and CH_3I. After the completion of the reaction, the mixture was diluted carefully with an aqueous solution of $KHSO_4$ (6.8 g, 50 mmol) and extracted with EA. The organic layer was additionally washed with $KHSO_4$ (5%), $NaHCO_3$ (5%), and brine, dried over Na_2SO_4, filtered and concentrated to dryness. The crude product was purified by flash chromatography (eluant: 1:3, EA/hexane) to give 5.63 g (22 mmol, 88%) of **7** as a colorless oil.

^{1}H NMR (400 MHz, $CDCl_3$) δ 5.68 (d, J = 0.7 Hz, 2H), 4.11 (qd, J = 7.1, 0.7 Hz, 4H), 1.27 (s, 12H), 1.22 (td, J = 7.1, 0.7 Hz, 6H). 13C{1H} NMR (101 MHz, $CDCl_3$) δ 176.4, 132.9, 60.5, 43.8, 25.0, 14.1. MS (ESI) calcd for $C_{14}H_{25}O_4^+$ $[M+H]^+$ *m/z* 257.1747, found 257.1906.

Compound 8 [2,2,5,5-tetramethylhex-3-(*E*)-enedioic acid]. Compound **7** (2.0 g, 7.8 mmol) was dissolved in THF (20 mL) and $LiOH \cdot H_2O$ (0.65 g, 15.6 mmol), dissolved in water (20 mL), was added dropwise. The reaction was stirred at 40°C overnight. The mixture was acidified with solid $KHSO_4$, and extracted with EA. The organic phase was dried over Na_2SO_4, filtered and concentrated to dryness to give compound **8** as a waxy solid (1.4 g, 7.02 mmol, 90%).

^1H NMR (400 MHz, DMSO) δ 12.22 (br, 2H), 5.65 (s, 2H), 1.19 (s, 12H). 13C{1H} NMR (101 MHz, DMSO) δ 177.7, 133.1, 43.6, 25.5. MS (ESI) calcd for $C_{10}H_{17}O_4^+$ $[M+H]^+$ *m/z* 201.1121, found 201.1279.

Compound 10 [isopropyl 5-[N-(tert-butyloxycarbonyl)amino]-2,2,5,5-tetramethyl-pent-3-(*E*)-enamide]. Compound **8** (1.0 g, 5 mmol) was dissolved in dry DCM and HOBt (0.34 g, 2.5 mmol) and EDC·HCl (0.48 g, 2.5 mmol) were added. After 15 min *i*Pr-NH_2 (237 µL, 2.76 mmol) was added to the reaction mixture, and DIPEA was used to reach basic pH. The reaction was allowed to stir overnight. The solvent was removed under reduced pressure and the residue dissolved in EA. The organic phase was washed with $KHSO_4$ (5%) and brine, dried over Na_2SO_4, filtered, and concentrated to dryness. The crude product was purified by flash chromatography (eluant: 2:3, EA/hexane) to give 0.53 g (2.2 mmol, 44%) of **9** [6-(isopropylamino)-6-oxo-2,2,5,5-tetramethylhex-3-(*E*)-enoic acid] as a colorless solid. Compound **9** (0.5 g, 2.07 mmol) was dissolved in dry THF and cooled with an ice bath. DIPEA (361 µL, 2.07 mmol) and DPPA (447 µL, 2.07 mmol) were added, and the solution was stirred for 30 min. Then, the ice bath was removed and the solution was allowed to reach room temperature. *t*-BuOH (10 mL) was added and the reaction was stirred under reflux overnight. The solvent was removed under reduced pressure and the residue dissolved in EA. The organic phase was washed with $KHSO_4$ (5%), $NaHCO_3$ (5%) and brine, dried over Na_2SO_4, filtered, and concentrated to dryness. The crude product was purified by

flash chromatography (eluant: 1:3, EA/hexane) to give 0.31 g (0.99 mmol, 48%) of **10** as a colorless solid.

Compound 9: ^{1}H NMR (400 MHz, $CDCl_3$) δ 5.87 (d, J = 4.5 Hz, 1H), 5.73 (q, 2H), 4.06 – 3.91 (m, 1H), 1.36 (s, 6H), 1.27 (s, 6H), 1.09 (d, J = 6.5 Hz, 6H). MS (ESI) calcd for $C_{13}H_{24}NO_3^+$ $[M+H]^+$ *m/z* 242.1750, found 242.1937.

Compound 10: Mp 131-133°C. ^{1}H NMR (400 MHz, $CDCl_3$) δ 6.60 (d, J = 6.3 Hz, 1H), 5.60 (q, 2H), 5.41 (s, 1H), 4.10 – 3.98 (m, 1H), 1.41 (s, 9H), 1.25 (s, 12H), 1.13 (d, J = 6.6 Hz, 6H). 13C{1H} NMR (101 MHz, $CDCl_3$) δ 175.5, 155.2, 134.1, 133.9, 54.1, 44.1, 41.3, 27.4, 25.1, 22.3, 21.5. IR (KBr) ν (cm^{-1}) 3328, 3251, 1698, 1645, 1530, 1458. MS (ESI) calcd for $C_{17}H_{33}N_2O_3^+$ $[M+H]^+$ *m/z* 313.2486, found 313.2673.

Compound 11 [isopropyl 5-[(azidocarbonyl)amino]-2,2,5,5-tetramethyl-pent-3-(*E*)-enamide]. This compound was recovered as a main secondary product from flash chromatography of the crude product in the synthesis of **10**. Yield: 12% (0.14 g, 0.49 mmol).

Mp 149-151°C. ^{1}H NMR (400 MHz, $CDCl_3$) δ 6.64 (d, J = 6.3 Hz, 1H), 5.65 (q, 2H), 5.41 (s, 1H), 4.07 (m, 1H), 1.44 (s, 6H), 1.29 (s, 6H), 1.17 (d, J = 6.6 Hz, 6H). IR (KBr) ν (cm^{-1}) 3353, 3303, 3253, 2132, 1694, 1644, 1525. MS (ESI) calcd for $C_{13}H_{24}N_5O_2^+$ $[M+H]^+$ *m/z* 282.1924, found 282.2111.

Conformational Energy Calculations. DFT calculations at the M06L/6-31+G(d,p) level[60] were performed in the gas phase. It should be noted that the M06L functional describes very satisfactorily the geometries and relative energies of conformations stabilized by electrostatic interactions and by π-electron-rich functional groups.[61] All quantum mechanics computations were carried out with the Gaussian09 software.[62] Frequency analyses were operated to verify the nature of the minimum state of all of the stationary points obtained and to calculate the zero-point vibrational energies (ZPVEs),

and both thermal and entropic corrections. These statistical terms were then used to compute the conformational Gibbs free energies in the gas phase (ΔG) at 298 K.

The conformational potential energy surface of each compound studied was systematically explored using a procedure inspired by the build-up method of Gibson and Scheraga.[63] This approach assumes that the short-range interactions are dominant in determining the conformation of a given peptide. Accordingly, the accessible conformations of any peptide studied result from combining *N* independent rotamers (*i.e*,. the rotational isomeric approximation[64]), in which each independent rotational state corresponds to the most favored conformation of each residue. In practice, accessible starting geometries for each compound were constructed by varying the free rotation backbone torsion angles (Scheme 1) in steps of 60°. Consequently, 6 (minima of φ) × 6 (minima of θ^1) × 6 (minima of θ^3) × 6 (minima of ψ) = 1296 minima were anticipated for the potential energy hypersurface $E = E(\varphi, \theta^1, \theta^3, \psi)$ of each *chiral* compound (*i.e.*, **C** and **D**). In the case of **A**, **B** and **E**, the number of theoretical minima can be reduced to 648 due to the absence of chirality, since structures with $(\varphi, \theta^1, \theta^3, \psi)$ and $(-\varphi, -\theta^1, -\theta^3, -\psi)$ are energetically degenerated and equivalent. Hence, 1296 × 2 (**C**, **D**) + 648 × 3 (**A**, **B**, **E**) structures were built and subsequently their geometries were optimized.

In order to construct a list of unique minima for each compound, all optimized geometries were compared and all unique minima found were ordered by a rank of increasing energy. We identify unique minimum energy conformations based on the values of the backbone torsion angles and the presence of interaction patterns (*i.e* , H-bonds between backbone amide groups). To facilitate the representation of the conformational space of the compounds in a simplified Ramachandran-like plot, two virtual torsion angles, defined as illustrated in Figure 2f, were selected to mimic the backbone torsion angles typically used for peptides based on α-amino acids. Each virtual rotation was chosen to account for the relative position of each amide group with respect to the central C=C double bond, which is a characteristic feature of all compounds investigated.

The validity of the two *virtual* torsion angles in reflecting the conformational properties of each compound was checked by comparing the clustering results with those achieved using the four main-chain torsion angles. The number of unique minima was identical for each case examined using both criteria. As for the analysis of the interactions, specific N–H···O H-bonds were defined to occur when the N-H···O distance is ≤ 3.0 Å and the ∠N–H···O angle is ≥ 120°.[65] Finally, two conformations were considered different when they diverge in at least one of their (*virtual*) torsion angles by more than 15° or in at least one of the interactions counted.

X-Ray Diffraction

Boc-5-aminopent-3-(E)-enoyl-NHiPr [(Boc)**A 6**]. Crystals of this compound were grown from EA – *n*-hexane by vapor diffusion at 4°C. X-Ray diffraction data were collected with a Gemini E four-circle kappa diffractometer (Agilent Technologies) equipped with a 92 mm EOS CCD detector, using graphite monochromated Cu Kα radiation (λ = 1.54184 Å). Data collection and reduction were performed with the CrysAlisPro software system (Rigaku Oxford Diffraction). A semi-empirical absorption correction based on the multi-scan technique using spherical harmonics, implemented in the SCALE3 ABSPACK scaling algorithm, was applied. The structure was solved by *ab initio* procedures of the SIR 2014 program.[66] The trial solution with the best combined figure of merit allowed location of three independent molecules in the monoclinic space group C2/c. Refinement was carried out by full-matrix least-squares on F^2, using all data, by application of the SHELXL-2014 program,[67] with anisotropic displacement parameters for all of the non-H atoms. Restraints were applied to the bond distances and angles of the terminal Boc and NH*i*Pr groups, as well as to the anisotropic displacement parameters of all atoms (RIGU command in SHELXL-2014). H-Atoms were calculated at idealized positions and refined using a riding model.

Boc-5-amino-2,2,5,5-tetramethyl-pent-3-(E)-enoyl-NHiPr [(Boc)**E 10**]. Crystals of this compound were grown from EA – petroleum ether by vapor diffusion. Data collection was performed on a

Philips PW1100 four-circle serial diffractometer in the θ-2θ scan mode using graphite monochromated Cu Kα radiation (λ = 1.54178 Å). The structure was solved by direct methods of the SIR 2002 program,[68] and refined by full-matrix least-squares on F^2, using all data, by application of the SHELXL-2014 program,[67] with anisotropic displacement parameters for all of the non-H atoms. H-Atoms were calculated at idealized positions and refined using a riding model.

Azidocarbonyl-5-amino-2,2,5,5-tetramethyl-pent-3-(E)-enoyl-NHiPr **11**. Crystals were grown from EA – petroleum ether by vapor diffusion. Data collection and reduction, structure solution and refinement were performed similarly to what reported above for the structure of (Boc)**A 6**. The C-terminal *i*Pr group is disordered. Its methyl groups were refined on two sets of positions (atoms CT2,CT3 and CT2',CT3', respectively), each with 0.50 population parameter. Restraints were applied to the bond distances, bond angles, and anisotropic displacement parameters of the disordered atoms.

Relevant crystal data and structure refinement parameters for the structures of **6**, **10**, and **11** are listed in Tables S6-S8 (Supporting Information). CCDC 1948908, 1948909, and 1952416 contain the supplementary crystallographic data for this paper. The data can be obtained free of charge from The Cambridge Crystallographic Data Centre *via* www.ccdc.cam.ac.uk/structures.

ACKNOWLEDGMENTS

D. Z. and C. A. acknowledge MINECO/FEDER (RTI2018-098951-B-I00) and the Agència de Gestió d'Ajuts Universitaris i de Recerca (2017SGR359). Support for the research of C. A. was received through the "ICREA Academia" prize for excellence in research funded by the Generalitat de Catalunya. Financial support to G. M. by CARIPARO Foundation (Ph.D. program, Padova, Italy), and to A. M. by the University of Padova (Grant PDiSC 06BIRD2018-UNIPD) is acknowledged. A. M. thanks Prof. J. W. Kelly as in his laboratory at the Department of Chemistry,

The Scripps Research Institute, La Jolla, CA, he began to work on the β,γ unsaturated δ-Ava residue. The Padova authors are grateful to Mr. Renato Schiesari for technical assistance in the FT-IR absorption experiments.

ASSOCIATED CONTENT

Supporting Information

The Supporting Information is available free of charge on the ACS Publications website at DOI: 10.1021/acs.joc.xxxxxxxx

- Computational details; X-ray crystal data, tables of torsion angles and H-bond parameters, packing diagrams for compounds **6**, **10**, and **11**; supporting FT-IR spectra; NMR characterization spectra for new compounds (PDF)
- X-Ray crystallography data of compounds **6**, **10**, and **11** (CIF)

AUTHOR INFORMATION

Corresponding Authors:

*E-mail: claudio.toniolo@unipd.it

alessandro.moretto.1@unipd.it

ORCID

Giulia Marafon: 0000-0002-6685-9489

Alessandro Moretto: 0000-0003-1563-9053

David Zanuy: 0000-0001-7704-2178

Carlos Alemán: 0000-0003-4462-6075

Marco Crisma: 0000-0003-3552-4106

Claudio Toniolo: 0000-0002-2327-1423

Notes

The authors declare no competing financial interest.

REFERENCES

(1) Ariëns, E. J. Receptors: From Fiction to Fact. *Trends Pharmacol.* **1979**, *1*, 11-15.

(2) Farmer, P. S.; Ariëns, E. J. Speculations on the Design of Nonpeptidic Peptidomimetics. *Trends Pharmacol. Sci.* **1982**, *3*, 362-365.

(3) Spatola, A. F. In *Chemistry and Biochemistry of Amino Acids, Peptides, and Proteins*; Weinstein, B., Ed.; Dekker: New York, NY, 1983; Vol. 7, pp 267-357.

(4) Mammen, M.; Shakhnovich, E. I.; Whitesides, G. M. Using a Convenient, Quantitative Model for Torsional Entropy To Establish Qualitative Trends for Molecular Processes That Restrict Conformational Freedom. *J. Org. Chem.* **1998**, *63*, 3168-3175.

(5) Lawson, A. D. G.; MacCoss, M.; Heer, J. P. Importance of Rigidity in Designing Small Molecule Drugs To Tackle Protein–Protein Interactions (PPIs) through Stabilization of Desired Conformers. *J. Med. Chem.***2018**, *61*, 4283-4289.

(6) Shamala, N.; Nagaraj, R.; Balaram, P. The 3_{10} Helical Conformation of a Pentapeptide Containing α-Aminoisobutyric Acid (Aib): X-Ray Crystal Structure of Tos-$(Aib)_5$-OMe. *J. Chem. Soc., Chem. Commun.* **1978**, 996-997.

(7) Toniolo, C.; Crisma, M.; Formaggio, F.; Peggion, C. Control of Peptide Conformation by the Thorpe-Ingold Effect (C^{α}-Tetrasubstitution). *Biopolymers (Pept. Sci.)* **2001**, *60*, 396-419.

(8) Raines, R. T.; Wennemers, H. Peptides on the Rise. *Acc. Chem. Res.* **2017**, *50*, 2419, and articles in this Special Issue on "Chemical Biology of Peptides".

(9) Gatto, E.; Quatela, A.; Caruso, M.; Tagliaferro, R.; De Zotti, M.; Formaggio, F.; Toniolo, C.; Di Carlo, A.; Venanzi, M. Mimicking Nature: A Novel Peptide-Based Bio-Inspired Approach for Solar Energy Conversion. *ChemPhysChem* **2014**, *15*, 64-68.

(10) Tiwari, P.; Basu, A.; Vij, A.; Bera, S.; Tiwari, A. K.; Dutt Konar, A. Rationally Designed Bioinspired δ-Amino Valeric Acid Based Hydrogel: One Shot Solution for Drug Delivery and Effluent Management. *Chem. Select* **2019**, *4*, 6896-6905.

(11) Banerjee, A.; Pramanik, A.; Bhattacharjya, S.; Balaram, P. Omega Amino Acids in Peptide Design: Incorporation into Helices. *Biopolymers* **1996**, *39*, 769-777.

(12) Baldauf, C.; Günther, R.; Hofmann, H.-J. δ-Peptides and δ-Amino Acids as Tools for Peptide Structure Design - A Theoretical Study. *J. Org. Chem.* **2004**, *69*, 6214-6220.

(13) Baldauf, C.; Hofmann, H.-J. *Ab initio* MO Theory – An Important Tool in Foldamer Research: Prediction of Helices in Oligomers of ω-Amino Acids. *Helv. Chim. Acta* **2012**, *95*, 2348-2383.

(14) Marafon, G.; Crisma, M.; Moretto, A. Intrinsically Photoswitchable α/β Peptides Toward Two-State Foldamers. *Angew. Chem. Int. Ed.* **2018**, *57*, 10217-10220.

(15) Marafon, G.; Crisma, M.; Moretto, A. Tunable *E*-*Z* Photoisomerization in α,β-Peptide Foldamers Featuring Multiple (*E*/*Z*)-3-Aminoprop-2-enoic Acid Units. *Org. Lett.* **2019**, *21*, 4182-4186.

(16) Veeresh, K.; Gopi, H. N. Design of Helical Peptide Foldamers through α,β → β,γ Double-bond Migration. *Org. Lett.* **2019**, *21*, 4500-4504.

(17) Devadder, S.; Verheyden, P.; Jaspers, H. C. M.; Van Binst, G.; Tourwé, D. The γ-Methyl-E-Olefin as Isosteric Replacement of the Peptide Bond. *Tetrahedron Lett.* **1996**, *37*, 703-706.

(18) Deschrijver, P.; Tourwé, D. Theoretical Conformational Analysis of Acetyl-Alanine-Methylamide Double Bond and Methyl-Substituted Double-Bond Isosteres of the Peptide Bond. *FEBS Lett.* **1982**, *146*, 353-356.

(19) Jakobsche, C. E.; Peris, G. Miller, S. J. Functional Analysis of an Aspartate-Based Epoxidation Catalyst with Amide-to-Alkene Peptidomimetic Catalyst Analogues. *Angew. Chem. Int. Ed.* **2008**, *47*, 6707–6711.

(20) Jakobsche, C. E.; Choudhary, A.; Miller, S. J.; Raines, R. n → π* Interaction and n)(π Pauli Repulsion Are Antagonistic for Protein Stability. J. *Am. Chem. Soc.* **2010**, 132, 6651-6653.

(21) Gardner, R. R.; Liang, G.-B.; Gellman, S. H. An Achiral Dipeptide Mimetic That Promotes β-Hairpin Formation. *J. Am. Chem. Soc.* **1995**, *117*, 3280-3281.

(22) Gardner, R. R.; Liang, G.-B.; Gellman, S. H. β-Turn and β-Hairpin Mimicry with Tetrasubstituted Alkenes. *J. Am. Chem. Soc.* **1999**, *121*, 1806-1816.

(23) Wipf, P.; Henninger, T. C.; Geib, S. J. Methyl- and (Trifluoromethyl)alkene Peptide Isosteres: Synthesis and Evaluation of Their Potential as β-Turn Promoters and Peptide Mimetics. *J. Org. Chem.* **1998**, *63*, 6088-6089.

(24) Liang, G.-B.; Dado, G. P.; Gellman, S. H. Anatomy of a Stable Intramolecularly Hydrogen Bonded Folding Pattern. *J. Am. Chem. Soc.* **1991,** *113*, 3994-3995.

(25) Liang, G.-B.; Desper, J. M.; Gellman, S. H. Effects of Backbone Rigidification on Intramolecular Hydrogen Bonding in a Family of Diamides. *J. Am. Chem. Soc.* **1993,** *115*, 925-938.

(26) Venkatachalam, C. M. Stereochemical Criteria for Polypeptides and Proteins. V. Conformation of a System of Three-Linked Peptide Units. *Biopolymers* **1968**, *6*, 1425-1436.

(27) Geddes, J. A.; Parker, K. B.; Atkins, E. D. T.; Beighton, E. "Cross-β" Conformation in Proteins. *J. Mol. Biol.* **1968**, *32*, 343-358.

(28) Toniolo, C. Intramolecularly Hydrogen Bonded Peptide Conformations. *CRC Crit. Rev. Biochem.* **1980**, *9*, 1-44.

(29) Rose, G. D.; Gierasch, L. M.; Smith, J. A. Turns in Peptides and Proteins. *Adv. Protein Chem.* **1985**, *37*, 1-109.

(30) Benedetti, E.; Bavoso, A.; Di Blasio, B.; Pavone, V.; Pedone, C.; Crisma, M.; Bonora, G. M.; Toniolo, C. Solid-State and Solution Conformation of Homo-Oligo (α-Aminoisobutyric

Acids) from Tripeptide to Pentapeptide: Evidence for a 3_{10} Helix. *J. Am. Chem. Soc.* **1982**, *104*, 2437-2444.

(31) Toniolo, C.; Benedetti, E. The Polypeptide 3_{10}-Helix. *Trends Biochem. Sci*. **1991**, *16*, 350-353.

(32) Karle, I. L.; Balaram, P. Structural Characteristcs of α-Helical Peptide Molecules Containing Aib Residues. *Biochemistry* **1990**, *29*, 6747-6756.

(33) Gessmann, R.; Brückner, H.; Petratos, K. Three Complete Turns of 3_{10}-Helix at Atomic Resolution: the Crystal Structure of Z-$(Aib)_{11}$-O*t*Bu. *J. Pept. Sci.* **2003**, *9*, 753-762.

(34) Solà, J.; Helliwell, M.; Clayden, J. Interruption of a 3_{10}-Helix by a Single Gly Residue in a Poly-Aib motif: a Crystallographic Study. *Biopolymers* **2011**, *95*, 62-69.

(35) Lizio, M. G.; Andrushchenko, V.; Pike, S. J.; Peters, A. D.; Whitehead, G. F. S.; Vitórica-Yrezábal, I. J.; Mutter, S. T.; Clayden, J.; Bouř, P.; Blanch, E. W.; Webb, S. J. Optically Active Vibrational Spectroscopy of α-Aminoisobutyric Acid Foldamers in Organic Solvents and Phospholipid Bilayers. *Chem. Eur. J.* **2018**, *24*, 9399-9408.

(36) Valle, G.; Crisma, M.; Formaggio, F.; Toniolo, C.; Jung, G. Geometry and Conformation of the α-Aminoisobutyric Acid Residue in Simple Derivatives and Peptides. Four New X-ray Structural Analyses and a Statistical Analysis from Known Crystal Data. *Liebigs Ann. Chem.* **1987**, 1055-1060.

(37) Beesley, R. M.; Ingold, C. K.; Thorpe, J. F. The Formation and Stability of *spiro*-Compounds. Part I. *spiro*-Compounds from Cyclohexane. *J. Chem. Soc.* **1915**, *107*, 1080-1105.

(38) Drouin, M.; Arenas, J. L.; Paquin, J.-F. Incorporating a Monofluoroalkene into the Backbones of Short Peptides: Evaluating the Impact on Local Hydrophobicity. *ChemBioChem* **2019**, *20*, 1817-1826.

(39) Frantz, M.-C.; Skoda, E. M.; Sacher, J. R.; Epperly, M. W.; Goff, J. P.; Greenberger, J. S.; Wipf, P. Synthesis of Analogs of the Radiation Mitigator JP4-039 and Visualization of BODIPY Derivatives in Mitochondria. *Org. Biomol. Chem.* **2013**, *11*, 4147-4153.

(40) Wipf, P.; Xiao, J. Convergent Approach to (*E*)-Alkene and Cyclopropane Peptide Isosteres. *Org. Lett.* **2005**, *7*, 103-106.

(41) Fu, Y.; Bieschke, J.; Kelly, J. W. *E*-Olefin Dipeptide Isostere Incorporation into a Polypeptide Backbone Enables Hydrogen Bond Perturbation: Probing the Requirements for Alzheimer's Amyloidogenesis. *J. Am. Chem. Soc.* **2005**, *127*, 15366-15367.

(42) Fu, Y.; Gao, J.; Bieschke, J.; Dendle, M. A.; Kelly, J. W. Amide-to-*E*-Olefin *versus* Amide-to-Ester Backbone H-Bond Perturbations: Evaluating the O-O Repulsion for Extracting H-Bond Energies. *J. Am. Chem. Soc.* **2006**, *128*, 15948-15949.

(43) Bieschke, J.; Siegel, S. J.; Fu, Y.; Kelly, J. W. Alzheimer's Aβ Peptides Containing an Isostructural Backbone Mutation Afford Distinct Aggregate Morphologies but Analogous Cytotoxicity. Evidence for a Common Low-Abundance Toxic Structure(s)? *Biochemistry* **2008**, *47*, 50-59.

(44) Hoffmann, R. W. Allylic 1,3-Strain as a Controlling Factor in Stereoselective Transformations. *Chem. Rev.* **1989**, *89*, 1841-1860.

(45) Yang, Y. In *Side Reactions in Peptide Synthesis*; Academic Press: London, 2015; pp. 110-113, and references therein.

(46) Benedetti, E.; Pedone, C.; Toniolo, C.; Némethy, G.; Pottle, M. S.; Scheraga, H. A. Preferred Conformation of the *tert*-Butoxycarbonylamino Group in Peptides. *Int. J. Pept. Protein Res.* **1980**, *16*, 156-172.

(47) Allen, F. H.; Kennard, O.; Watson, D. G.; Brammer, L.; Orpen, A. G.; Taylor, R. Tables of Bond Lengths determined by X-Ray and Neutron diffraction. Part 1. Bond Lengths in Organic Compounds. *J. Chem. Soc., Perkin Trans. II* **1987**, S1-S19.

(48) Chakrabarti, P.; Dunitz, J. D. Structural Characteristics of the Carboxylic Amide Group. *Helv. Chim. Acta* **1982**, *65*, 1555-1562.

(49) Ramakrishnan, C.; Prasad, N. Study of Hydrogen Bonds in Amino Acids and Proteins. *Int. J. Protein Res.* **1971**, *3*, 209-231.

(50) Taylor, R.; Kennard, O.; Versichel, W. Geometry of the N-H···O=C Hydrogen Bond. 1. Lone-Pair Directionality. J. *Am. Chem. Soc.* **1983**, *105*, 5761-5766.

(51) Taylor, R.; Kennard, O.; Versichel, W. The Geometry of the N-H···O=C Hydrogen Bond. 3. Hydrogen-Bond Distances and Angles. *Acta Crystallogr. B* **1984**, *40*, 280-288.

(52) Görbitz, C. H. Hydrogen-Bond Distances and Angles in the Structures of Amino Acids and Peptides. *Acta Crystallogr. B* **1989**, *45*, 390-395.

(53) Metrano, A. J.; Abascal, N. C.; Mercado, B. Q.; Paulson, E. K.; Hurtley, A. E.; Miller, S. J. Diversity of Secondary Structure in Catalytic Peptides with β-Turn-Biased Sequences. *J. Am. Chem. Soc.* **2017**, *139*, 492-516.

(54) Avignon, M.; Huong, P. V.; Lascombe, J.; Marraud, M.; Néel, J. Étude, par Spectroscopie Infra-Rouge, de la Conformation de Quelques Composés Peptidiques Modèles. *Biopolymers* **1969**, *8*, 69-89.

(55) Pysh, E. S.; Toniolo, C. Conformational Analysis of Protected Norvaline Oligopeptides by High Resolution Proton Magnetic Resonance. *J. Am. Chem. Soc.* **1977**, *99*, 6211-6219.

(56) Baron, M. H.; de Lozé, C.; Toniolo, C.; Fasman, G. D. Structure in Solution of Protected Homo-Oligopeptides of L-Valine, L-Isoleucine, and L-Phenylalanine: An Infrared Absorption Study. *Biopolymers* **1978**, *17*, 2225-2239.

(57) Kennedy, D. F.; Crisma, M.; Toniolo, C.; Chapman, D. Studies of Peptides Forming 3_{10}- and α-Helices and β-Bend Ribbon Structures in Organic Solution and in Model Biomembranes by Fourier Transform Infrared Spectroscopy. *Biochemistry* **1991**, *30*, 6541-6548.

(58) Toniolo, C.; Crisma, M.; Moretto, A.; Peggion, C.; Formaggio, F.; Alemán, C.; Cativiela, C.; Ramakrishnan, C.; Balaram, P. Peptide δ-Turn: Literature Survey and Recent Progress. *Chem. Eur. J.* **2015**, *21*, 13866-13877.

(59) Kopple, K. D.; Ohnishi, M.; Go, A. Conformations of Cyclic Peptides. IV. Nuclear Magnetic Resonance Studies of *cyclo*-Pentaglycyl-L-Leucyl and *cyclo*-Diglycyl-L-Histidyldiglycyl-L-Tyrosyl. *Biochemistry* **1969**, *8*, 4087-4095.

(60) Zhao, Y.; Truhlar, D. G. A New Local Density Functional for Main-Group Thermochemistry, Transition Metal Bonding, Thermochemical Kinetics, and Noncovalent Interactions. *J. Chem. Phys.* **2006**, *125*, 194101-194118.

(61) Wanga, Y.; Jina, X.; Yub, H. S.; Truhlar, D. G.; He, X. Revised M06-L Functional for Improved Accuracy on Chemical Reaction Barrier Heights, Noncovalent Interactions, and Solid-State Physics. *Proc. Natl. Acad. Sci. USA* **2017**, *114*, 8487–8492.

(62) Frisch, M. J.; Trucks, G. W.; Schlegel, H. B.; Scuseria, G. E.; Robb, M. A.; Cheeseman, J. R.; Scalmani, G.; Barone, V.; Mennucci, B.; Petersson, G. A.; Nakatsuji, H.; Caricato, M.; Li, X.; Hratchian, H. P.; Izmaylov, A. F.; Bloino, J.; Zheng, G.; Sonnenberg, J. L.; Hada, M.; Ehara, M.; Toyota, K.; Fukuda, R.; Hasegawa, J.; Ishida, M.; Nakajima, T.; Honda, Y.; Kitao, O.; Nakai, H.; Vreven, T.; Montgomery, J. A., Jr.; Peralta, J. E.; Ogliaro, F.; Bearpark, M.; Heyd, J. J.; Brothers, E.; Kudin, K. N.; Staroverov, V. N.; Kobayashi, R.; Normand, J.; Raghavachari, K.; Rendell, A.; Burant, J. C.; Iyengar, S. S.; Tomasi, J.; Cossi, M.; Rega, N.; Millam, J. M.; Klene, M.; Knox, J. E.; Cross, J. B.; Bakken, V.; Adamo, C.; Jaramillo, J.; Gomperts, R.; Stratmann, R. E.; Yazyev, O.; Austin, A. J.; Cammi, R.; Pomelli, C.; Ochterski, J. W.; Martin, R. L.; Morokuma, K.; Zakrzewski, V. G.; Voth, G. A.; Salvador, P.; Dannenberg, J. J.; Dapprich, S.; Daniels, A. D.; Farkas, O.; Foresman, J. B.; Ortiz, J. V.; Cioslowski, J.; Fox, D. J. *Gaussian 09*, Revision A.01. Gaussian, Inc.: Wallingford, CT, 2009.

(63) Gibson, K. D.; Scheraga, H. A. Revised Algorithms for the Build-Up Procedure for Predicting Protein Conformations by Energy Minimization. *J. Comput. Chem.* **1987**, *8*, 826-834.

(64) Flory P. J. *Statistical Mechanics of Chain Molecules*; Interscience Publishers: New York, NY, 1969.

(65) Teixeira-Dias, B.; Zanuy, D.; Poater, J.; Solà, M.; Estrany, F.; del Valle, L. J.; Alemán, C. Binding of 6-Mer Single-Stranded Homo-Nucleotides to Poly(3,4-Ethylenedioxythiophene): Specific Hydrogen Bonds with Guanine. *Soft Matter* **2011**, *7*, 9922-9932.

(66) Burla, M. C.; Caliandro. R.; Carrozzini, B.; Cascarano, G. L.; Cuocci, C.; Giacovazzo, C.; Mallamo, M.; Mazzone, A.; Polidori, G. Crystal Structure Determination and Refinement *via SIR2014*. *J. Appl. Crystallogr.* **2015**, *48*, 306-309.

(67) Sheldrick, G. M. Crystal Structure Refinement with SHELXL. *Acta Crystallogr. C* **2015**, *71*, 3-8.

(68) Burla, M. C.; Camalli, M.; Carrozzini, B.; Cascarano, G. L.; Giacovazzo, C.; Polidori, G.; Spagna, R. SIR2002: The Program. *J. Appl. Crystallogr.* **2003**, *36*, 1103.

For Table of Contents Only